Chain conformation in ultrathin polymer films

Ronald L. Jones*[a], Christopher L. Soles[a], Francis W. Starr[a], Eric K. Lin[a], Joseph L. Lenhart[a], Wen-Li Wu[a], Dario L. Goldfarb[b], Marie Angelopoulos[b]; [a]National Institute of Standards and Technology; [b]IBM T.J. Watson Research Center

ABSTRACT

Using Small Angle Neutron Scattering (SANS), we present the first quantitative measurements of the 3-dimensional conformation of macromolecules in thin polymer films of $D < R_{G,Bulk}$, where D is the film thickness and $R_{G,Bulk}$ is the bulk radius of gyration. For $D \approx 0.5\ R_{G,Bulk}$, the molecular size along the film normal is less than $0.5\ R_{G,Bulk}$, while relatively small changes are observed parallel to the surface. The observed changes in molecular size agree with predictions of molecular dynamics simulations of polymers confined in thin films, resulting from increased molecular orientation rather than chain distortion. Segregation of molecular centers of mass to the film center facilitates molecular packing while minimizing chain distortion. Estimates of length scales relating to the onset of chain distortion and chain orientation in thin film resists are $D \approx 0.1R_{G,Bulk}$ and $D \approx N\sigma$ respectively, where D is the film thickness, N is the number of chain segments, and σ is the persistence length.

1. INTRODUCTION

As film thickness approaches the molecular dimensions, polymer shape and size are expected to become thickness dependent, affecting properties such as polymer solubility, modulus, permeability, and optical properties. The thicknesses of photoresists planned for sub-100 nm lithography may approach this limit, however a lack of experimental data precludes an accurate estimation of the relevant length scales. The distortion of chain conformation is typically suspected whenever material properties deviate from bulk values at $D \approx R_{G,Bulk}$, where D is the film thickness and $R_{G,Bulk}$ is the molecular radius of gyration in the bulk melt. Numerous reports of thickness dependent properties include substrate wettability [1], segmental mobility [2-4], diffusivity of small molecule penetrants [5,6], and thermal expansion [7,8]. According to Reiter [9], the thickness dependent density in thin film lubricants results from changes in molecular packing, consistent with the observation of increased segmental orientation [10-12]. In addition to a reduction in chain size normal to the surface, elongation parallel to the surface can result in anisotropic properties. The presence of anisotropy in chain shape could play a role in reported polymer self-diffusion coefficients [13-15]. In thin films, chain self-diffusion coefficients are reduced in all directions, however diffusion along the surface normal proceeds at rates orders of magnitude lower than within the surface plane. The length scale of this anisotropy has been associated with the contour length of the chain, where the first effects of chain confinement are expected [13].

Polymer molecules are often approximated as spherical blobs, however Silverberg [16] calculated the average shape as ellipsoidal with an aspect ratio of nearly 14 [16, 17]. Within a thin film, numerous simulations predict the rotation of the long axis parallel to the surfaces, allowing the molecules to retain their bulk shape [18-21]. In contrast, theoretical descriptions of polymers based on absorbtion predict an abundance of flattened conformations at surfaces [22], resulting in reduced entanglement [23]. While the shape and size of molecules within thin films has been debated for many years, experimental determinations of molecular shape and size as a function of confinement have been limited due, in part, to the extremely small sample volumes required. Shuto *et al.* [24] measured conformation in stacks of multiple films on a single substrate. The study used Small Angle Neutron Scattering (SANS) to measure films as thin as $0.1\ R_{G,Bulk}$, reporting significant increases in molecular size within the plane of the films. In that study, films could not be annealed, however similar effects were observed using off-specular neutron reflectivity [25] where annealing is possible. In contrast, recent extensions of SANS measurements to individual films demonstrate a lack of significant change (< 15%) in the R_G measured parallel to the substrate, consistent with theoretical predictions [26,27]. SANS measurements were

* Ronald.Jones@nist.gov; [a] Polymers Division, National Institute of Standards and Technology, 100 Bureau Dr. MS 8541, Gaithersburg, MD 20899-8541; [b] IBM T.J. Watson Research Center, P.O. Box 218, Yorktown Heights, NY 10598

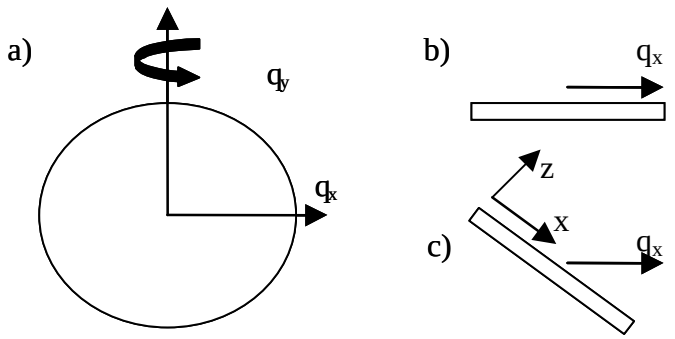

Figure 1. Scattering vector, q, relative to the substrate geometry. Shown in (a) are the components of the scattering vector, q_x and q_y, parallel to the substrate surface when $\theta=0^o$. The direction of rotation is also indicated, demonstrating a lack of rotation around q_y. When the beam is normal to the substrate (b), both q_x and q_y are parallel to the substrate, while rotation about q_y produces information along both the x- and z-axis (c). The y-axis in both (b) and (c) is perpendicular to the page.

previously limited to determinations of R_G along 2-dimensions, however molecular dimensions along the surface normal can be inferred from surface-directed density waves measured by specular reflectivity [28,29]. Decreasing wavelengths are associated with reduced molecular dimensions, supporting a flattened or reduced molecular size along the film normal, however there is no analogous measurement of bulk samples.

We present an extension of prior SANS measurements by Jones et al. [27] to include information in all three dimensions of a polymer film. The films serve as a model system for all amorphous polymer films with weak interaction (i.e. physadsorbtion) between the polymer and substrate. The results are interpreted in terms of the ratio of film thickness to bulk R_G. In this way, the results can be applied to a wide array of resists using bulk data on molecular dimensions. In contrast to prior studies using SANS and reflectivity, the scattering vector is controlled by rotation of the sample in the neutron beam, providing information both parallel and perpendicular to the substrate. Data from thin films with a total thickness less than $R_{G,Bulk}$ are compared to analogous bulk data. The data are modeled using the Kratky limit of the structure factor of a 3-dimensional Gaussian chain. To establish the validity of the Kratky model in thin films, we simulate the effects of confinement on the structure factor using molecular dynamics simulations. These simulations also provide insight into the real-space molecular packing. To our knowledge, this represents the first simultaneous measurement of molecular shape and size within a thin film in all three dimensions.

2. METHODOLOGY

2.1 Sample Preparation

Nine films of deutero-poly(styrene) (dPS) and poly(styrene) (PS), where the dPS mass fraction is [0.50 ± .02], were spin cast from solution onto silicon substrates. Polymers were purchased from Polymer Source, Inc. [30] with weight average relative molecular mass, $M_{w,r}$, of 398,000 ($M_{w,r}/M_{n,r}$=1.12) and 380,000 ($M_{w,r}/M_{n,r}$=1.04) for the dPS and PS respectively. Blends were prepared by dissolution in toluene and spin cast on cleaned silicon substrates. Substrates were polished, SEMI standard, 150 mm diameter, ultra-high grade silicon, purchased from Silicon, Inc. Substrates were cleaned prior to spin casting with oxygen plasma for [5 ± 0.1] m [31]. The oxide layer was stripped by immersion in a buffered hydrofluoric acid etch ([5 to 6] vol. % HF, [10 to 11] vol. % NH_4F in water) and subsequently regrown in a standard UV/Ozone cleaner. All films were simultaneously annealed at [150 ± 5] °C for more than 12 h, exceeding estimates of the relaxation time and quenched to room temperature. The film thickness, determined through x-ray reflectometry, of all nine films was [10.8 to 11.3] nm, with a standard deviation in film-to-film thickness on the order of the error in the film thickness measurement. The surface roughness was consistently [0.5 to 1.0] nm. The films were checked for homogeneity using a Digital Instruments Nanoscope III atomic force microscope (AFM) and found to be

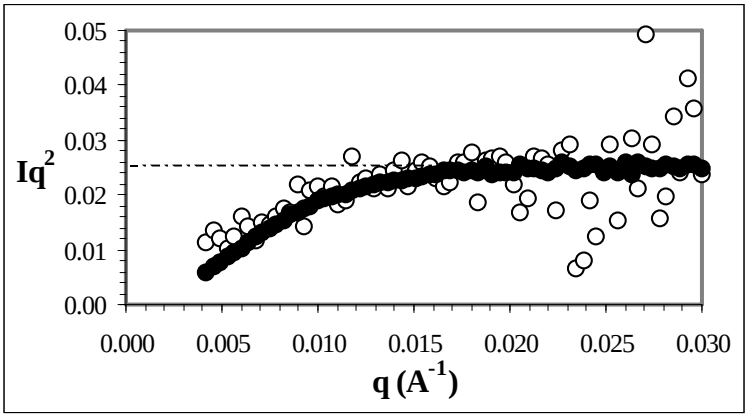

Figure 2. Kratky plot of SANS data from a bulk sample (filled circles) and a stack of 11nm thin films in the unrotated ($\theta=0^o$) configuration. The horizontal asymptote indicated by the dashed line is used to extract the persistence length according to equation 1.

free of flaws characteristic of dewetting [9]. A bulk sample of the same composition was cast from solution in toluene and allowed to air dry before annealing at [150 ± 2] °C for 3 h under vacuum to remove residual solvent. Samples were then mechanically pressed to a uniform thickness (ca. 0.2 mm) and annealed under the conditions outlined for films.

2.2 SANS Data Analysis

SANS measurements were performed at the NIST Center for Neutron Research (Gaithersburg, MD) on the NG-3 30 m beam line. The neutron wavelength, λ, was set to 0.8 nm with a wavelength spread, $\Delta\lambda/\lambda$, of 0.11 to avoid Bragg diffraction from the silicon substrates. The collimation was set using a 19 mm circular aperture at the sample, a pre-sample flight path of approximately 10.0 m (4 guides), and a sample-detector distance of [10.8 ± 0.01] m. The intensity is collected on a 2-dimensional detector and then corrected for dark current, scattering from the sample cell, and detector efficiency using standard algorithms. Sample cell scattering is determined from measuring nine blank wafers (i.e. without polymer films) in both the rotated and non-rotated geometry. To reduce the background scattering, the experiments were performed under vacuum. Intensities are normalized by sample volume and subsequently reduced to an absolute scale relative to a standard sample of known neutron cross section measured under the same configuration. While the large diameter substrates permit the rotation of films without beam spillover, the increased beam footprint increases the sample volume probed. The projected beam footprint is approximated as a rectangle of dimensions L x Lcos(θ), where L is the circular aperture diameter. The increased footprint is then incorporated during data reduction through volume normalization of intensity. The q-independent incoherent scattering was determined by similar measurement of bulk samples of pure PS and dPS and subtracted from the blend data according to standard procedures. The detector was offset along the q_x-axis (see figure below) by 10 cm, providing a maximum scattering vectors q_x = 0.5 $Å^{-1}$ and q_y = 0.2 $Å^{-1}$ along the y-axis.

The high neutron transparency of silicon allows measurements of films in transmission. For all measurements, nine films are stacked in series to increase the signal/noise ratio. In contrast to prior experiments, the measurements reported here consist of two sample orientations relative to the neutron beam (see fig. 1). In describing these measurements, we employ two separate coordinate systems based on the detector (q_x, q_y, q_z, where the q_x-q_y plane is always parallel to the detector surface) and the sample surface (x,y,z, where the x-y plane is always parallel to the film surface). In the first case, the beam is perpendicular to the substrate surface, and the x-y plane is parallel to the q_x-q_y plane. In the second orientation, the q_x-axis is placed at an angle of [63 ± 5]^o to the x-axis of the surface. Note that in this configuration, the q_y-axis remains parallel to the y-axis. In the cases of isotropic scattering, data is circularly averaged at constant $q_r=(q_x^2+q_y^2)^{1/2}$, producing a radially averaged intensity. In the case of rotated samples, circular averaging was not performed due to anisotropy of the scattering pattern. Instead, the intensity along the two axes are defined by $I(q_x)=I(q_x,q_y=0)$ and $I(q_y)=I(q_y,q_x=0)$.

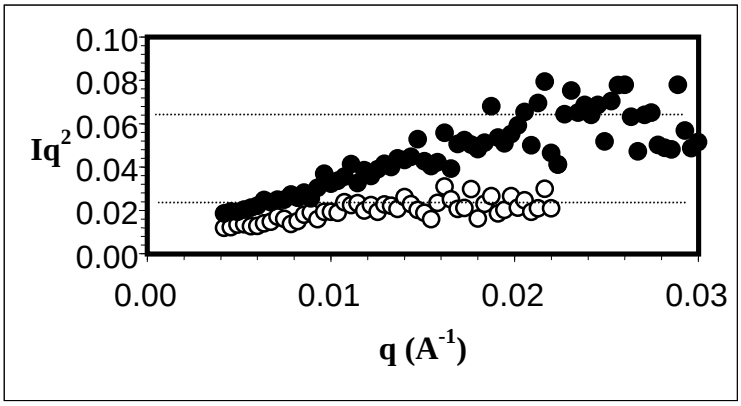

Figure 3. SANS data from 11nm films plotted in Kratky form. Data are shown from averages along the q_x axis (filled circles) and qy axis (open circles). Horizontal asymptotes, from which segmental lengths are calculated as described in the text, are indicated by dotted lines.

The persistence length, σ_p, is calculated in the Kratky limit ($qR_G>1$) for a 3-dimensional Gaussian chain using …

$$I(q) = b_v \nu \phi(1-\phi)\sigma_p^{-2} q^{-2} \qquad (1)$$

where I(q) is the measured coherently scattered intensity as a function of q, b_v is the neutron contrast factor, ϕ is the volume fraction of the deuterated polymer, and ν is the segmental molar volume. The neutron contrast factor calculated from standard tables for dPS/PS is b_v =[4.16e-3 ± 0.02] cm^4/mole while the molar volume of styrene is reported as [=100.4 mol/cm^3] [34]. The segment length provides the 3-dimensional averaged radius of gyration through the scaling relationship $\langle R_G^2\rangle = N\sigma^2/6$, where N is the number average molecular weight. $\langle R_G^2\rangle$ can be projected along any of the Cartesian axes by vector addition, namely $\langle R_G^2\rangle = \langle R_{Gx}^2\rangle + \langle R_{Gy}^2\rangle + \langle R_{Gz}^2\rangle$. For an isotropic system, all vectorial components are equivalent, and the total size results from, for example, its x-axis projection by $\langle R_G^2\rangle = 3\langle R_{Gx}^2\rangle$. In an anisotropic system, the three directions are not equivalent and must be individually measured. Based on the geometry of figure 1, $I(q_x)$ and $I(q_y)$ are interpreted separately by equation (1), resulting in values of $\langle R_G^2\rangle$ representing $3\langle R_{Gqx}^2\rangle$ and $3\langle R_{Gqy}^2\rangle$ respectively. For $\theta=0^o$, $\langle R_{G,qx}^2\rangle$ and $\langle R_{G,qy}^2\rangle$ are both parallel to the plane of the film. Rotation of the film to $\theta=63^o$ yields $\langle R_{G,\theta=63}^2\rangle = 3\langle R_{G,qx}^2\rangle$, where $\langle R_{G,\theta=63}^2\rangle$ has components both parallel and perpendicular to the substrate.

2.3 Additional Sources of Scattered Intensity

The reliable measurement of coherent scattering resulting from molecular conformation requires an accounting of alternative sources of background intensity. In addition to parasitic scattering from the sample cell, the rotation of the films potentially introduces scattering from structural components with finite dimensions perpendicular to the substrates, namely scattering resulting from surface segregation and correlations between the two surfaces. The structural scattering resulting from two infinite planes is only significant near the condition $\theta=90^o$, where the reciprocal planes intersect the Ewald sphere. For liquid films, the correlations of the top surface to bottom surface can contribute to off-axis scattering [30]. To address this possible factor, a similar stack of pure dPS films were measured under identical conditions at θ = 63º. The measured scattering, collected over 12 hours, was indistinguishable from that of the empty cell and was not further considered. While the contribution of surface segregation to the coherent scattering could not be rigorously determined, the extent of surface segregation, measured on the NG-7 neutron reflectometer, was found to be negligible. The lack of surface segregation is consistent with the observations of Hariharan *et al.* for films with $D < 2R_{G,Bulk}$ [32].

2.4 Simulation Model

Our findings are based on molecular dynamics simulations of an ultra-thin polymer film confined between moderately attractive smooth surfaces, as well as simulations of a pure melt for comparison purposes. We use a well-studied bead-spring model [33] that models polymers as chains of monomers. All monomer pairs interact via a Lennard-Jones (LJ) potential V_{LJ}, and bonded monomers along a chain are connected via a FENE anharmonic spring potential

$$V_{FENE}(r) = -k(R_0^2/2) \ln (1-(r/R_0)^2),$$

where r is the distance between neighboring monomers. As with many prior studies, we set constant k=30 and R_0=1.5. This model captures essential polymer properties, but ignores chemical details that are unnecessary to gain a general understanding of structural changes resulting from confinement. Since we do not aim to study a specific polymer, we present our results in "reduced units", where length is in units of σ (σ is the LJ length parameter) and temperature is in units ε/k_B (ε is the LJ energy parameter and k_B is Boltzmann's constant). The potential between monomers and the wall is defined by the "9-3" LJ potential $V_{wall}(z) = \varepsilon_w[(\sigma/z)^9 - (\sigma/z)^3]$, where z is the distance of a monomer from the wall and ε_w=0.5. This form corresponds to an infinitely thick wall of uniformly dense particles interacting with the normal 12-9 LJ potential.

A cell of dimensions L_x=L_y=50 and L_z =4 containing 107 chains of 70 monomers each with periodic boundary conditions parallel to the surface. The chain length used is slightly larger than the entanglement length. We consider both thin film and bulk systems with a constant average density of ≈1. Monomers are initially configured along a lattice, which is heated to high temperature (T=8.0) to allow the system to relax any artifacts from arbitrary initial conditions. We subsequently cool the system to T=2.0 and record configurations at this temperature. This temperature is chosen sufficiently far from the glass transition temperature, T_g, to ensure equilibration.

3. RESULTS

The molecular dimensions parallel to the surfaces of a thin film are compared to the analogous bulk measurement in figure 2. From equation 1, the q-independent asymptote for the bulk sample indicates a persistence length, σ_p = [0.68 ± 0.01] nm, in agreement with prior reports for polystyrene melts [34], and $\langle R_G^2 \rangle^{1/2}$ = [16.3 to 16.7] nm for the 11 nm films. In the limit of q=0, the scattering vector is primarily in the plane of the sample along both the q_x and q_y axes. The Kratky asymptotes yield σ_p =[0.68 ± 0.03] nm and $\langle R_G^2 \rangle^{1/2}$ = [16.5 ± 0.6] nm and are equivalent to the bulk values. These results are consistent with prior observations using similar samples and the same sample configuration. Rotation of the sample to θ=63˚ does not affect the orientation of the q_y axis relative to the y-axis, and the measured structure factor is expected to match the θ=0˚ data. This consistency is observed from thin films in the θ=63º geometry, where $I(q_y)$ agrees with I(q) at θ=0º (see figure 3). We note that limits on detector placement decrease the maximum available q_y relative to the radially averaged data sets, thereby increasing the uncertainty of the segmental length determination at high q. Therefore, a fitted value for σ is not reported from the data along q_y, however $I(q_y)$ is observed to overlay I(q) from the bulk sample over the entire q-range. Within the context of an estimated 15% experimental error in the Kratky asymptote, we cannot rule out small changes in molecular size parallel to the substrate, and we therefore focus on the dimensions perpendicular to the substrate.

In the limit of large θ, the $\langle R_G^2 \rangle$ obtained from $I(q_x)$ is dominated by the molecular dimensions perpendicular to the substrate. This configuration measures the real space projection of molecular dimensions on the vector defined by θ = 63º. The measured persistence length represents a similar projection of average segmental length, and is necessarily connected in the usual manner to chain flexibility. Given that projections of isotropic molecules are, by definition, independent of θ, the disparity of σ as a function of q is in itself a measure of molecular anisotropy. In figure 3, the value of σ results in a molecular size of $\langle R_{G,\sigma=63^o}^2 \rangle^{1/2}$ = [10.4 ± 0.8] nm, representing a reduction of nearly 40% from $R_{G,Bulk}$.

The results presented thus far depend on the connection of the increased scattering at large q vectors to the reduction in molecular dimensions in a thin film. While this is a plausible hypothesis based on the Kratky limit, equation (1) is

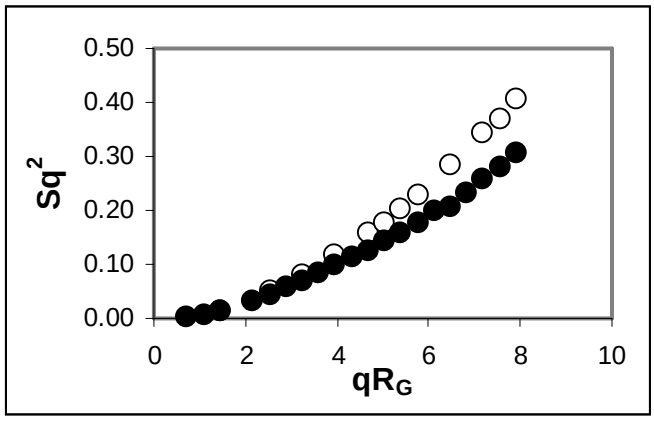

Figure 4. Predicted structure factor, S(q), from molecular dynamics simulations plotted in Kratky form for two sample orientations. Shown are results from θ=0º (solid circles) and θ=63º (open circles).

strictly derived for bulk systems. We have therefore simulated the effects of confinement on the structure factor for a model system to test our interpretation. Using molecular dynamics simulations, the structure factor of a thin polymer film both within the plane of the surfaces and at an angle of θ = 63˚ is presented in figure 4. As in the experimental measurements, increased intensity at large q is observed in the rotated configuration resulting from decreased molecular size. In addition, simulations predict a constant intercept in the limit of q = 0, where I(q = 0) is proportional to the Flory-Huggins interaction parameter. The constancy of I(q = 0) suggests that factors affecting segregation, miscibility, and solubility are not affected in the sub-R_G regime. Unfortunately, experimental determination of I(q = 0) in thin films remains elusive due to a variety of technical issues, however, to our knowledge this prediction has not been previously reported. Increased intensities predicted at larger q vectors are, however, consistent with the increased Kratky asymptote observed in figure 3.

Decreases in $\langle R_G^2 \rangle^{1/2}$ measured perpendicular to the surface can originate from either distortion of the chain or rotation of the ellipsoids along the surface. Following the model used in the SANS data reduction, components of R_G measured in the plane parallel ($R_{G||} = 3/2 \langle R_{G,xy}^2 \rangle^{1/2}$) and perpendicular ($R_{G\perp} = 3\langle R_{Gz}^2 \rangle^{1/2}$) to the substrate are given in figure 4 as a function of distance from the substrate. Molecules with centers of mass near either surface are predictably elongated, increasing in size by as much as 40 % in the first few layers, while those located near the film center are closer to the bulk average. With the majority of chains located near the central plane of the film, the volume averaged R_G is within the 20 % error associated with SANS determinations of R_G. A much larger effect is found perpendicular to the substrate, as $R_{G\perp} \approx 0.5\ R_{G,Bulk}$ in the film interior. The relative magnitudes of these effects serve to explain the lack of change in the R_G measured at θ=0º with large changes observed at θ=63º.

As in the experimental measurements, an isotropic system is defined by the equivalence of the vector components, resulting in the condition $R_{G,||} = R_{G,\perp} = R_{G,Bulk}$. In figure 4, the projected molecular dimensions are no longer equivalent in all three dimensions, increasing parallel to the substrate with a resultant decrease normal to the surface. However, vector addition of the components ($\langle R_{Gx}^2 \rangle^{1/2} + \langle R_{Gy}^2 \rangle^{1/2} + R_{Gz}^2 \rangle^{1/2}$) yields a value of the 3-dimensional average R_G that is consistent with bulk dimensions. Near the surfaces, even the 3-dimensional average RG increases, suggesting that the chains are highly elongated, however the average molecule retains a bulk shape and size. This result demonstrates the propensity to rotate rather than distort. A compression of the chains would result in a 3-dimensional average less than the bulk average, and would suggest either a loss of interpenetration or an increase in film density.

The persistence of bulk conformation in sub-R_G films due to the rotation of asymmetric ellipsoids at the surface suggests a new length scale of confinement. Based on the ratios predicted by Wei and Eichinger [17], confinement is expected to produce true molecular deformation when $D \approx 0.1\ R_{G,Bulk}$. For common photoresists, where $R_{G,Bulk}$ is typically 1-3 nm,

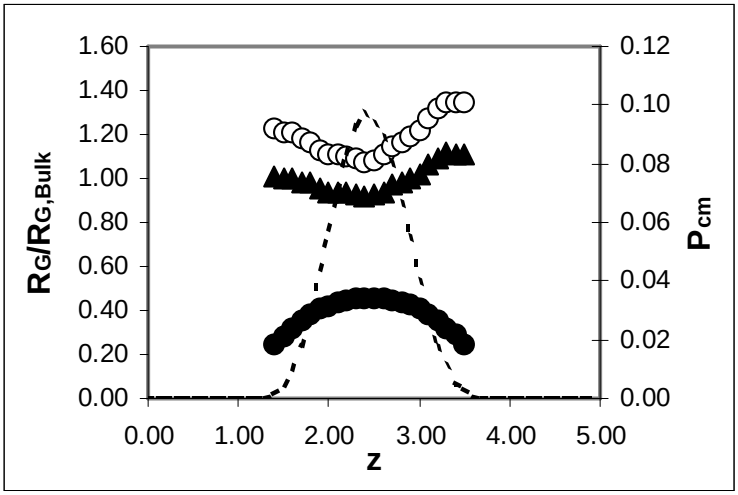

Figure 5. Molecular size in the thin film, R_G, relative to the bulk, $R_{G,Bulk}$, as a function of distance from the solid substrate, z. Shown are data for thin film R_G measured as a projection along the surface (open circles), and along the surface normal (filled circles). Also shown is the 3-dimensional value of R_G (filled triangle). The probability density of the molecular center of mass, Pcm, is plotted (dotted line) showing the relative location of chain centers within the film.

this length scale implies bulk properties in even atomically thin resists. While these results do not support significant chain deformation in ultrathin films, they do suggest measurable changes in chain orientation. In contrast to chain deformation, rotation of the ellipsoids is expected whenever confinement reduces the total number of possible conformations. The largest conformation possible is the stretched chain, suggesting the initial onset of orientation in films as thick as the contour length of the polymer ($\sim N\sigma$). At this length scale, the infinitesimal number of affected conformations would result in a lack of measurable deviations from bulk behavior, however we note the findings on anisotropic self-diffusion coefficients propagating to these length scales [gast, lin]. Decreasing film thickness would then serve to increase the number of ellipsoids required to rotate and hence the degree of orientation. For resist films, the length scale of confinement is therefore conservatively estimated on the order of 100 - 300 nm, however the thickness dependence of orientation will require direct measurement of films with varying thickness.

5. CONCLUSIONS

The 3-dimensional conformation of a model polymer system has been measured in an ultrathin film, where the film thickness is approximately a quarter of the average chain diameter ($D \approx 0.5\ R_{G,Bulk}$). Data indicate that the chain dimensions perpendicular to the substrate are significantly reduced from bulk values, while the conformation parallel to the substrate is bulk-like. The measured form factor agrees qualitatively with predictions from molecular dynamics simulations of freely-jointed polymers in a thin film on a weakly interacting substrate. Analysis of the simulated conformations reveals that the molecules maintain their bulk conformations while orienting their long-axis along the surfaces. Based on these results, the feature dimensions required to truly flatten the chains were estimated to be on the order of the short axis of Guassian chains, approaching the length scales of individual segments. Predictions for intensity in the limit q = 0, corresponding to the compressibility of the polymer, is the same parallel and perpendicular to the surfaces, reflecting that angle dependent changes in scattering are purely structural and not thermodynamic in origin. The resulting length scales associated with chain orientation is the chain contour length, $D \approx N\sigma$, while chain deformation is only expected when film thickness approaches the smallest dimensions of the average ellipsoidal chain, namely $D \approx 0.1\ R_{G,Bulk}$.

ACKNOWLEDGMENTS

This work was funded in part by DARPA, contract N66001-00-C-8803. Joseph L. Lenhart is grateful to the National Research Council for postdoctoral funding.

REFERENCES

1. W. Zhao, M.H. Rafailovich, J. Sokolov, L.J. Fetters, R. Plano, M.K. Sanyal, S.K. Sinha, B.B. Sauer, "Wetting Properties of Thin Liquid Polyethylene Propylene Films", *Phys. Rev. Lett.*, **70**, 1453-1456, 1993.
2. C.L. Soles, J.F. Douglas, W.-L. Wu, R.M. Dimeo, "Incoherent Neutron Scattering and the Dynamics of Confined Polycarbonate Films", *Phys. Rev. Lett.*, **88**, 037401(1-4), 2002.
3. W.E. Wallace, D.A. Fischer, K. Efimenko, W.-L. Wu, J. Genzer, "Polymer Chain Relaxation: Surface Outpaces Bulk", *Macromolecules*, **34**, 5081-5082, 2001.
4. S. Rivillon, P. Auroy, B. Deloche, "Chain Segment Order in Polymer Thin Films on a Nonadsorbing Surface: A NMR Study", *Phys. Rev. Lett.*, **84**, 499-502, 2000.
5. K.C. Tseng, N.J. Turro, C.J. Durning, "Molecular Mobility in Polymer Thin Films", *Phys. Rev. E*, **61**, 1800-1811, 2000.
6. D.S. Fryer, P.F. Nealy, J.J. de Pablo, "Scaling of Tg and Reaction Rate with Film Thickness in Photoresist: A Thermal Probe Study", *J. Vac. Sci. Technol. B*, **18**, 3376-3380, 2000.
7. J.A. Forrest, K. Dalnoki-Veress, J.R. Dutcher, "Interface and Chain Confinement effects on the Glass Transition Temperature of Thin Polymer Films", *Phys. Rev. E*, **56**, 5705-5716, 1997.
8. R.A.L. Jones, "Dynamics in thin polymer films", *Curr. Opin. Colloid In.*, **4**, 153-158, 1999.
9. G. Reiter, "Dewetting as a Probe of Polymer Mobility in Thin Films", *Macromolecules*, **27**, 3046-3052, 1994.
10. V.J. Novotny, I. Hussla, J.-M. Turlet, M.R. Philpott, "Liquid Polymer Conformation on Solid Surfaces", *J. Chem. Phys.*, **90**, 5861-5868, 1989.
11. M.M. Despotopoulou, R.D. Miller, J.F. Rabolt, C.W. Frank, "Polymer Chain Organization and Orientation in Ultrathin Films: A Spectroscopic Investigation", *J. Polym. Sci. Part B.*, **34**, 2335-2349, 1996
12. G. Leclerc, J.J. Pireaux, R. Caudano, C. Honings, H. Hocker, "Higher Resolution Electron Energy Loss Sectroscopy Investigation of Molecular Conformation at the Surface of Poly(amino acid)s Films", *J. Chem. Phys.*, **101**, 781-787, 1994.
13. B. Frank, A.P. Gast, T.P. Russell, H.R. Brown, C. Hawker, "Polymer Mobility in Thin Films", *Macromolecules*, **29**, 6531-6534, 1996.
14. X. Zheng, M.H. Rafailovich, J. Sokolov, Y. Strzhemechny, S.A. Schwarz, B.B. Sauer, M. Rubenstein, "Long-Range Effects on Polymer Diffusion Induced by a Bounding Interface", *Phys. Rev. Lett.*, **79**, 241-244, 1997.
15. E.K. Lin, R. Kolb, S.K. Satija, W.-L. Wu, "Reduced Polymer Mobility near the Polymer/Solid Interface as Measured by Neutron Reflectivity", *Macromolecules*, **32**, 3753-3757, 1999
16. A. Silberberg, "Distribution of Conformations and Chain ends near the Surface of a Melt of Linear Flexible Macromolecules", *J. Coll. Int. Sci.*, **90**, 86-91, 1982.
17. G. Wei, B.E. Eichinger, "Shape Distributions for Gaussian Molecules: Circular and Linear Chains as Asymmetric Ellipsoids", *Macromolecules*, **23**, 4845-4855, 1990
18. I. Bitsanis, G. Hadziioannou, "Molecular Dynamics Simulations of the Structure and Dynamics of Confined Polymer Melts", *J. Chem. Phys.*, **92**, 3827-3847, 1990.
19. A.E. van Giessen, I. Szleifer, "Monte Carlo Simulations of Chain Molecules in Confined Environments", *J. Chem. Phys.*, **102**, 9069-9076, 1995.
20. S.K. Kumar, M. Vacatello, D. Yoon, "Off-lattice Monte Carlo simulations of polymer melts confined between 2 plates", *J. Chem. Phys.*, **89**, 5206-5215, 1988.
21. C. Mischler, J. Baschnagel, S. Dasgupta, K. Binder, "Structure and Dynamics of Thin Polymer Films: A Case Study with the Bond-Fluctuation Model", *Polymer*, **43**, 467-476, 2002.
22. "Polymers at Interfaces", G.J. Fleer, M.A. Cohen Stuart, J.M.H.M. Scheutjens, T. Cosgrove, B. Vincent, Chapman and Hall, London, 1993.
23. "Scaling Concepts in Polymer Physics", P.G. deGennes, Cornell Press, 1982.

24. K. Shuto, Y. Oishi, T. Kajiyama, C.C. Han, "Aggregation structure of a 2-dimensionally ultrathin polystyrene film prepared by the water casting method", *Macromolecules*, **26**, 6589-6594, 1993.
25. J. Kraus, P. Müller-Buschbaum, T. Kuhlmann, D.W. Schubert, M. Stamm, "Confinement effects on the chain conformation in thin polymer films", *Europhys. Lett.*, **49**, 210-216, 2000.
26. R.L. Jones, S.K. Kumar, D.L. Ho, R.M. Briber, T.P. Russell, "Chain Conformation in Ultrathin Polymers using Small Angle Neutron Scattering", *Macromolecules*, **34**, 559-565, 2001.
27. R.L. Jones, S.K. Kumar, D.L. Ho, R.M. Briber, T.P. Russell, "Chain Conformation in Ultrathin Polymer Films", *Nature* **400**, 146-148, 1999.
28. G. Evmenenko, S.W. Dugan, J. Kmetko, P. Dutta, "Molecular Ordering in Thin Liquid Films of Polydimethylsiloxanes", *Langmuir*, **17**, 4021-4024, 2001.
29. M. Tolan, O.H. Seeck, J. Wang, S.K. Sinha, M.H. Rafailovich, J. Sokolov, "X-ray Scattering from Polymer Films", *Physica B*, **283**, 22-26, 2000.
30. Commercial equipment and materials are identified in this paper only to adequately specify experimental procedure. In no case does this imply endorsement or recommendation by the National Institute of Standards and Technology.
31. The data throughout this manuscript, in the figures, and in the tables are presented along with the standard uncertainty (±) involved in the measurement.
32. A. Hariharan, S.K. Kumar, M. Rafailovich, J. Sokolov, X. Zheng, D.H. Duong, S.A. Schwarz, T.P. Russell, "The effect of finite film thickness on surface segregation in symmetrical binary polymer mixtures", *J. Chem. Phys.*, **99**, 656-663, 1993.
33. H.R. Warner, "Kinetic Theory and rheology of dilute suspensions of finitely extendible dumbbells", *Ind. Eng. Chem. Fundam.*, **11**, 379-387, 1972.
34. J.D. Londono, A.H. Narten, G.D. Wignall, K.G. Honnell, E.T. Hsieh, T.W. Johnson, F.S. Bates, "Composition dependence of the interaction parameter in isotopic polymer blends", *Macromolecules*, **27**, 2864-2871, 1994.